Development 137, 2265-2278 (2010) doi:10.1242/dev.044826

Modeling bistable cell-fate choices in the *Drosophila* eye: qualitative and quantitative perspectives

Thomas G. W. Graham[1], S. M. Ali Tabei[2], Aaron R. Dinner[2] and Ilaria Rebay[1,*]

Summary

A major goal of developmental biology is to understand the molecular mechanisms whereby genetic signaling networks establish and maintain distinct cell types within multicellular organisms. Here, we review cell-fate decisions in the developing eye of *Drosophila melanogaster* and the experimental results that have revealed the topology of the underlying signaling circuitries. We then propose that switch-like network motifs based on positive feedback play a central role in cell-fate choice, and discuss how mathematical modeling can be used to understand and predict the bistable or multistable behavior of such networks.

Key words: Yan, Mathematical modeling, Multistable switch, Photoreceptor development, Signaling network

Introduction

The development of a multicellular organism requires a coordinated sequence of individual cell-fate decisions. Many of these decisions appear to be binary: life or death, proliferation or quiescence, epidermal or neuronal fate, lymphoid or myeloid progenitor (Heitzler and Simpson, 1991; Albeck et al., 2008; Laslo et al., 2008; Yao et al., 2008). Binary choices are typically made by bistable switches, which are biochemical mechanisms that can reside stably in either of two dynamic steady states (reviewed by Ferrell, 2002). This review focuses on the role that bistable switches play in a classic model of cell-fate choice: the eye of the fruit fly *Drosophila melanogaster*. Just as signal transduction pathways have proven to be highly conserved and extensively deployed, the underlying design principles of the switches used in the fly eye will almost certainly be broadly relevant to understanding animal development. We discuss how understanding these general design principles and how they are employed in specific cases will benefit from approaches that combine quantitative experimental techniques with mathematical modeling.

The *Drosophila* eye has served for many years as a valuable experimental system for studying complex cell-fate choices. The adult eye is a highly ordered array of ~800 repeated units called ommatidia. Each ommatidium contains 20 cells arranged in precisely the same configuration, although with opposite chirality in the dorsal and ventral halves of the eye. The highly stereotyped configuration of each ommatidium arises from an initially uniform primordium of undifferentiated, unpatterned cells, termed the eye imaginal disc. Starting in late larval stages, a signaling wave sweeps across the disc from posterior to anterior, initiating the development of evenly spaced ommatidia (Fig. 1A). Recruitment of cell types into each ommatidium occurs in a specific sequence of inductive, rather than lineage-based, interactions (see Fig. 1B), beginning with the eight photoreceptor neurons and followed by the non-neuronal cone and pigment cells (Ready et al., 1976).

Rather than providing a comprehensive review of cell-fate specification during fly eye development [for more information on this topic, please see reviews by Moses (Moses, 2002) and Roignant and Treisman (Roignant and Treisman, 2009)], we discuss several examples of genetic networks in the *Drosophila* eye that are thought to mediate specific bistable cell-fate decisions. Although qualitative genetic analyses have provided critical insight into the function and topology of these circuits, further quantitative experimentation and mathematical modeling will be needed to achieve a deeper understanding of the connection between network dynamics and observable cellular behaviors. In this vein, we present two original hypotheses in the form of mathematical models. Our goal in presenting these new models in the context of a review article is to provide a new perspective on existing experimental results, to illustrate a general form that future models of the systems in question might take, and to provide a starting point for suggesting future directions for coordinated experimental and modeling approaches.

Quantitative models can describe development at various levels of detail, from the action of individual proteins and genes to the behavior of cells within tissues. Although there have been some striking successes in connecting morphogenesis to mathematical descriptions of chemical reaction-diffusion systems (Turing, 1952; Sick et al., 2006), quantitative developmental biology is only now emerging in earnest [see, for example, the accompanying review in this issue by Grimm et al. on modeling the Bicoid gradient (Grimm et al., 2010) and reviews by Meinhardt (Meinhardt, 2008), Oates et al. (Oates et al., 2009) and Montell (Montell, 2008)]. In part, this shift reflects the advent of better experimental tools for studying development, but it also reflects the need to integrate information about many different molecular players to obtain an understanding of phenotypes and developmental processes at the systems level. We discuss how simple mathematical models can be used to understand why certain networks exhibit bistability. We then review several putative bistable networks involved in cell-fate choice in the *Drosophila* eye and demonstrate how one of these networks can be described using a more detailed mathematical model. Finally, we consider how switch-like motifs might be combined to form more complex multistable networks, and we illustrate two possible strategies by presenting a new hypothesis regarding a classic series of cell-fate choices during *Drosophila* eye development.

An introduction to bistable switches

A regulatory network exhibits bistability when a graded stimulus gives rise to one of two discrete steady states rather than to a continuum of responses. The first experimental work supporting the idea that bistable switches in biochemical networks could encode binary cellular decisions came from studies of gene

[1]Ben May Department for Cancer Research and [2]James Franck Institute, University of Chicago, 929 East 57th Street, Chicago, IL 60637, USA.

*Author for correspondence (irebay@uchicago.edu)

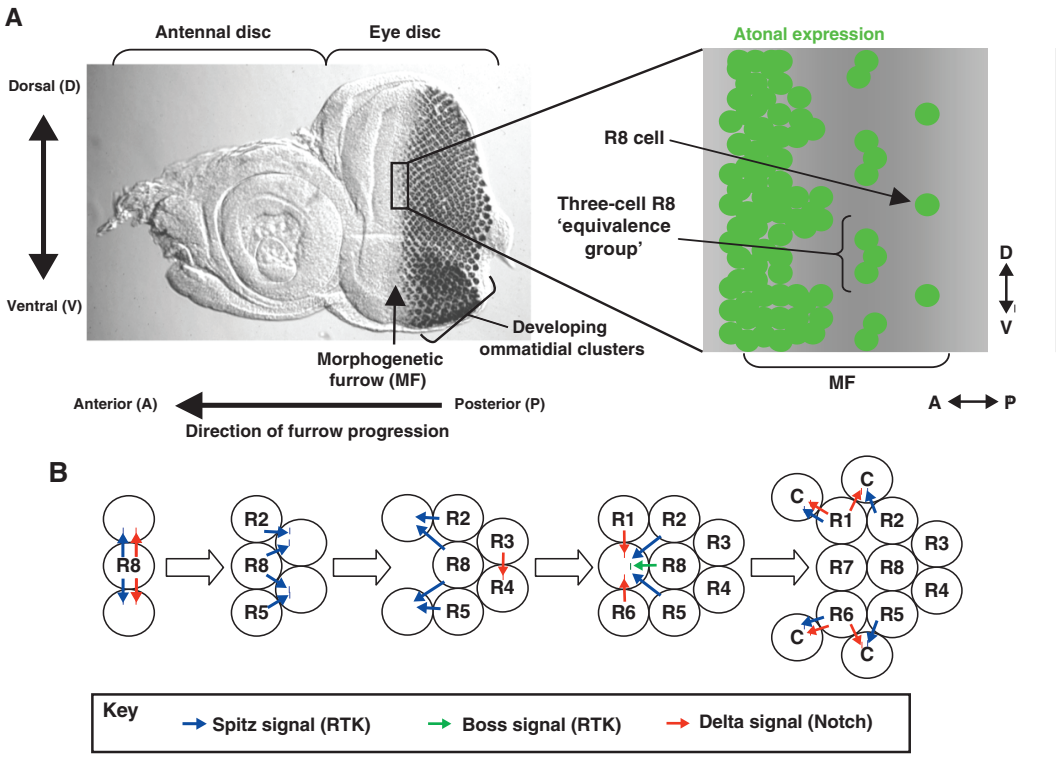

Fig. 1. Overview of pattern formation and cell-fate choice in the *Drosophila* eye. (**A**) A Nomarski micrograph of a developing third instar larval eye antennal imaginal disc labeled with an antibody to the nuclear photoreceptor marker Elav. A wave of signaling and photoreceptor recruitment associated with a visible indentation in the tissue, the morphogenetic furrow (MF), sweeps across the disc from posterior to anterior. An initial row of R8 'founder cells' is recruited at the posterior edge of the MF, followed by the sequential recruitment of the additional cell types of each ommatidium. Thus, more posteriorly located ommatidia are in more advanced stages of development. To the right is an illustration of the expression pattern of the transcription factor Atonal (Ato) (green) in the vicinity of the MF. Lateral inhibition signaling gradually resolves a broad pattern of Ato expression at the anterior edge of the MF into individual R8 progenitor cells. Adapted with permission from Voas and Rebay (Voas and Rebay, 2004). (**B**) A simplified schematic showing the sequence of inductive signaling events leading to the specification of photoreceptors (R8; R2, R5; R3, R4; R1, R6; R7) and cone cells (C) within a single ommatidium. Colored arrows represent different signaling events, whereas the large white arrows indicate the progression of time. The receptor tyrosine kinase (RTK) ligand Spitz is produced by differentiated photoreceptors to induce the differentiation of subsequent cell types (blue arrows).

regulation in *Escherichia coli* that showed how alternate high and low expression states of the *lac* operon could be stably maintained by positive feedback mediated through induction of the lactose permease LacY (Novick and Weiner, 1957). A second class of switch, involving mutual repression between a pair of genes, was first proposed as a thought experiment by Monod and Jacob (Monod and Jacob, 1961), and was later validated as the molecular mechanism responsible for the lysis versus lysogeny decision in bacteriophage λ (reviewed by Ptashne, 2004). The phage λ and *lac* operon switches have since been the subject of extensive quantitative experimental and theoretical work (Ackers et al., 1982; Reinitz and Vaisnys, 1990; Wong et al., 1997; Arkin et al., 1998; Setty et al., 2003; Bintu et al., 2005; Santillán and Mackey, 2004; Saiz et al., 2005; Elf et al., 2007; Kuhlman et al., 2007; Choi et al., 2008).

More recently, bistable switches have been described in multiple contexts in both prokaryotes and eukaryotes (Ferrell, 2002; Dubnau and Losick, 2006). For example, in *Drosophila*, positive feedback in binding of the Decapentaplegic (Dpp) protein to its receptor is thought to give rise to bistability during early embryonic dorsoventral patterning (Wang and Ferguson, 2005; Umulis et al., 2006), whereas positive feedback between the Dpp and Epidermal growth factor receptor (Egfr) pathways has been proposed to generate bistable responses during wing vein patterning (Yan et al., 2009). Switch-like network behavior has also been implicated in sharpening segmental gene expression boundaries in the early *Drosophila* embryo (Edgar et al., 1989; Lopes et al., 2008) and, as will be discussed in this review, in specifying a variety of cell fates in the fly eye.

Crucial to every bistable switch is some form of nonlinear positive feedback (Cinquin and Demongeot, 2002; Ferrell, 2002; Graf and Enver, 2009; Huang, 2009; Siegal-Gaskins et al., 2009; Warmflash and Dinner, 2009). It has been shown experimentally that a very simple bistable switch can be built from a single factor that positively regulates itself (Becskei et al., 2001; Kramer and Fussenegger, 2005). Such bistability can be understood using an equation that describes the rate (dx/dt) at which the concentration of the protein product (x) changes with time based on its rates of production [g(x)] and degradation (bx):

$$dx / dt = g(x) - bx . \quad (1)$$

An often-used form for g(x) is the Hill function, an expression that can describe cooperativity in which the dose-response curve increases more sharply than it would with a single ligand-receptor

binding event, often leading to a threshold-like behavior [see, for instance, Rosenfeld et al. (Rosenfeld et al., 2005) and Setty et al. (Setty et al., 2003)]:

$$g(x) = x^n / (x^n + k^n) . \quad (2)$$

The exponent in this expression (n), known as the Hill coefficient, is a measure of the cooperativity of the response. We will use Hill functions here and in later sections of this review to model the induction or repression of a gene by a transcription factor.

The steady-state solutions of equation (1) are given by setting $dx/dt=g(x)–bx=0$, and are represented graphically by the intersection of the curves $z=g(x)$ and $z=bx$ (Fig. 2A). For the choices of g(x) and b in Fig. 2A, there are three such intersections, implying three values of x for which x is unchanging. Consider the intersection at $x=x_3$. If we perturb the system slightly by adding more x, the degradation rate bx becomes greater than the production rate g(x), and the concentration of x will decrease until $bx=g(x)$ at $x=x_3$. The opposite will happen if we perturb the system by decreasing x. Thus, $x=x_3$ represents a stable state, or attractor, of the system, as the system returns to $x=x_3$ when slightly perturbed. By the same token, $x=x_1$ is also an attractor. By contrast, at $x=x_2$, the addition of a bit more x causes the production rate to exceed the degradation rate. Amplification of the initial small perturbation will continue until the system reaches the next stable state, $x=x_3$. Conversely, at $x=x_2$, a small reduction in x causes the degradation rate to exceed the production rate, such that x will decrease until it reaches $x=x_1$. Thus, $x=x_2$ is an unstable state of the system. The stability of extreme states and the instability of intermediate states are defining characteristics of bistable switches.

Positive feedback may also be indirect (Gardner et al., 2000). Consider a system of two genes, x and y, that repress each other. This situation can be modeled using two equations:

$$dx / dt = f_1(y) – b_1x , \quad (3)$$

$$dy / dt = f_2(x) – b_2y , \quad (4)$$

where $f_1(y)$ and $f_2(x)$ are decreasing functions of y and x, and b_1 and b_2 are first-order rate constants for x and y degradation, respectively. Stationary solutions of x and y occur when dx/dt and dy/dt both equal zero and are shown graphically as the intersection between the curves $f_1(y)=b_1x$ and $f_2(x)=b_2y$ in Fig. 2B. As before, two stable attractors [(x_1,y_1) and (x_3,y_3)] are separated by an unstable steady state (x_2,y_2).

Although nonlinear positive feedback within a genetic circuit is a necessary condition for bistability, it is not sufficient. The network model represented in Fig. 2C, despite having the same topology as the network in Fig. 2B, has only one stable steady-state solution. Varying a single parameter, in this case the response threshold for regulation of one gene by the protein product of another, can thus make the difference between whether a network functions as a bistable switch or not. This example illustrates how the behavior of bistable networks cannot be rigorously described by exclusively qualitative analyses of positive-feedback circuits, but rather requires elucidation of the quantitative relationships between network components. Indeed, a single regulatory network can be monostable at one developmental stage and bistable at another (Laslo et al., 2006).

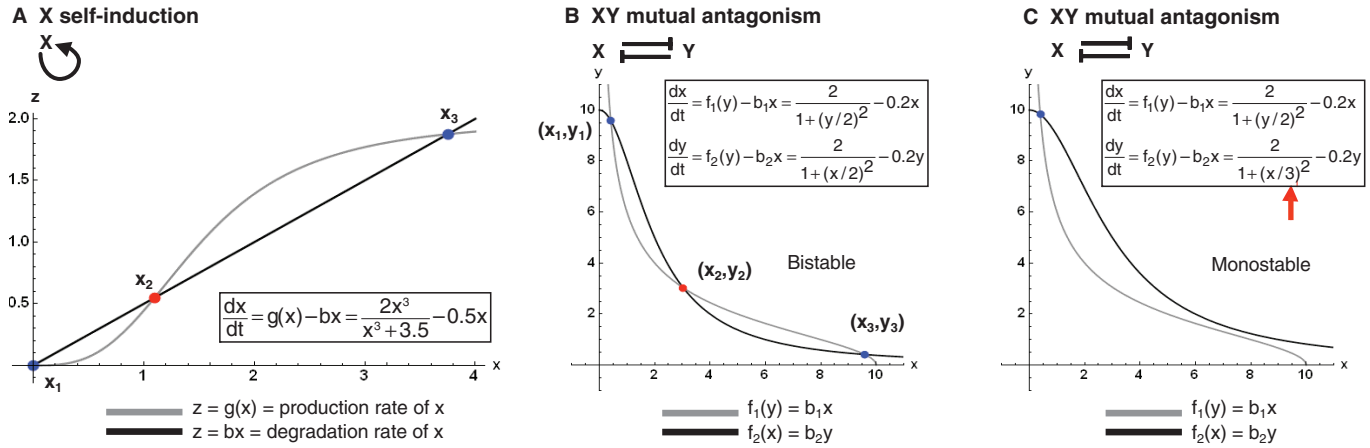

Fig. 2. Mathematical models of bistability. (**A**) A bistable switch may be built from a single protein (X) that induces its own expression (curved arrow). To model this self-induction, the production rate of X is taken here to be an increasing Hill function of the concentration of X. Plotted on the graph are rates of production (gray) and degradation (black) of X (vertical axis) as a function of the concentration of X (horizontal axis). Steady states (red and blue points) exist where the production rate of X [g(x)] is equal to its degradation rate (bx). These steady states may be stable (blue) or unstable (red). The difference in the X production and degradation rates will cause the system to return to the stable points following small perturbations. However, small perturbations from the unstable point will tend to be amplified, causing the system to 'run away' from the unstable point towards one of the two stable points. (**B**) A bistable switch may also be built from two factors (X and Y) that repress the production of each other. Here, this mutual antagonism is represented mathematically by modeling the production rate of one factor as a decreasing Hill function of the concentration of the other factor. The horizontal and vertical axes of the plot correspond to concentrations of X and Y, respectively, and the gray and black curves are the solutions to the steady-state equations $dx/dt=0$ and $dy/dt=0$, respectively. The intersections between these two curves represent steady-state points at which the concentrations of both X and Y are unchanging. As in A, two of these steady states are stable, whereas the intermediate steady state is unstable. (**C**) An alternative choice of parameters for the network in B (red arrow) can reduce the number of stable solutions to one, turning a bistable network into a monostable network. This emphasizes that the behavior of bistable networks depends crucially on the quantitative details of interactions within the network.

Below, we discuss several putative bistable switches involved in cell-fate choice in the *Drosophila* eye. Although each contains a source of positive feedback, which is a necessary ingredient for bistability, an important future direction for experimentation and modeling will be to determine whether the quantitative aspects of known interactions within each network are indeed sufficient to produce bistable behavior.

Putative bistable switches for cell-fate choice in the *Drosophila* eye

Subtype choice within R8: a two-component switch

R8 photoreceptors differentiate into subtypes that express different light-sensitive rhodopsin proteins (Fig. 3A). Coordination between R8 cells and neighboring R7 cells gives rise to distinct classes of ommatidia that express different pairs of rhodopsins (Franceschini et al., 1981). In so-called pale ommatidia, R7 cells express Rhodopsin 3 (Rh3), whereas R8 cells express Rh5. In so-called yellow ommatidia, R7 and R8 cells express Rh4 and Rh6, respectively. Genetic results suggest that the pale versus yellow decision results from a stochastic choice within R7 that is subsequently communicated to R8 (Chou et al., 1996; Chou et al., 1999; Wernet et al., 2006; Bell et al., 2007).

Although very little is known about how the R7 cell informs the R8 cell of its pale versus yellow decision (Birkholz et al., 2009), recent work has revealed that this choice is maintained in R8 by a bistable switch involving mutual antagonism between the NDR family kinase Warts (Wts) and the pleckstrin homology (PH) domain protein Melted (Melt) (Mikeladze-Dvali et al., 2005; Morante et al., 2007; Johnston and Desplan, 2008). Loss-of-function alleles of *wts* or *melt* convert all R8 cells into the pale or yellow subtypes, respectively. Conversely, pan-neuronal expression of Wts or Melt converts almost all R8 cells into the yellow or pale subtypes, respectively (Mikeladze-Dvali et al., 2005). Despite these dramatic effects on pale versus yellow fate choice in R8, *wts* and *melt* mutant alleles have no effect on pale versus yellow fate choice in R7. Neither does clonal loss of either factor in R7 influence the pale versus yellow specification of the neighboring R8 cell. Analysis of *wts* and *melt* transcriptional reporters reveals a complementary pattern of expression in R8 cells that corresponds to the two different subtypes. The two reporters are also induced or repressed in mutant backgrounds in the directions that would be expected if Wts and Melt repress each other at a transcriptional level. Collectively, these results imply that mutually antagonistic transcriptional regulation between Wts and Melt acts cell-autonomously in R8 to direct specification of pale versus yellow subtypes (Fig. 3A) (Mikeladze-Dvali et al., 2005).

Because Wts and Melt are not transcription factors, their mutual repression must be indirect (Mikeladze-Dvali et al., 2005). It will therefore be interesting to identify the transcriptional effectors acting downstream of Wts and Melt in this context. Results with mutants of *hippo* and *salvador*, two other components of the canonical Wts pathway, suggest that the same pathway through which Wts regulates cell proliferation might also be important in the pale versus yellow cell-fate choice (Mikeladze-Dvali et al., 2005). However, a role for Yorkie, the canonical transcriptional effector of Wts pathway signaling, has not yet been reported, nor have transcriptional effectors of Melt, such as Foxo (Teleman et al., 2005), yet been implicated in the decision.

The R8 versus R2/5 decision

Ommatidial differentiation begins with the selection of evenly spaced R8 founder cells flanked by presumptive R2 and R5 cells (Fig. 1A and Fig. 3B). Experimental results reveal at least two key sources of positive feedback that could give rise to bistability in the choice between R8 and R2/5: mutual activation by the transcription factors Senseless (Sens) and Atonal (Ato), and mutual antagonism between Sens and the transcription factor Rough (Ro).

The pattern of R8 recruitment is dictated by a complicated sequence of events that regulate the expression pattern of Ato. Inductive Notch and Dpp signaling initially induce a zone of *ato* expression across the anterior ridge of the morphogenetic furrow (Jarman et al., 1994; Jarman et al., 1995; Baker et al., 1996; Baker and Yu, 1997; Baonza and Freeman, 2001). Notch-mediated lateral inhibition, in conjunction with Egfr signaling, then resolves the broad stripe of *ato* expression into a series of evenly spaced three-cell clusters, known as the R8 equivalence group (Baker and Zitron, 1995; Dokucu et al., 1996; Frankfort et al., 2001) (see Fig. 1A and Fig. 3B). During this stage, Ato induces expression of *sens*, which feeds back to positively regulate *ato*. Eventually, *ato* expression is resolved to a single cell. In a recent mathematical model of this patterning process, the Ato/Sens positive-feedback loop was proposed to play a central role as a bistable switch for the

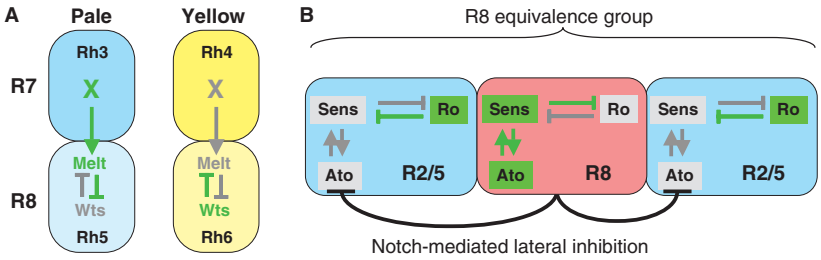

Fig. 3. Two intracellular bistable cell-fate switches in *Drosophila* eye development. (**A**) The pale versus yellow switch. Pale and yellow subtypes of the R7 and R8 photoreceptors are distinguished by expression of different light-sensitive rhodopsin (Rh) proteins. Within R8, the signaling molecules Warts (Wts) and Melted (Melt) exhibit mutual transcriptional antagonism via a presumably indirect mechanism that has yet to be elucidated. Melt expression promotes the pale subtype in R8, whereas Wts expression promotes the yellow subtype. An upstream pale versus yellow cell-fate decision in the neighboring R7 cell influences the Wts/Melt switch in R8 via an unknown juxtacrine signal (X). Active components and connections are green, whereas inactive ones are gray. Relatively well-established connections are shown by solid lines; in other figures, poorly understood or speculative interactions are shown by dotted lines. (**B**) The R2/5 versus R8 switch in the R8 equivalence group of cells (see Fig. 1A). The R8 and R2/5 cell-fate determinants Senseless (Sens) and Rough (Ro) repress each other cell-autonomously. Sens is also engaged in a mutual-activation loop with the transcription factor Ato, the expression of which is initially refined to a single cell per cluster through Notch-mediated lateral inhibition.

all-or-none specification of R8 cells (Pennington and Lubensky, 2010). Cells in which the Ato switch has been flipped to a high-Ato state produce an inhibitory signal that represses *ato* expression in adjacent cells, while also producing an activator that diffuses faster than the inhibitor to promote the recruitment of the next row of evenly spaced founder cells. This elegant 'switch and template' mechanism is thus proposed to exploit the interplay between intracellular bistable switches and long-range extracellular signals to generate a tissue-scale pattern.

Despite the importance of the Ato/Sens positive-feedback loop, it functions only transiently, as *ato* expression is lost in developing R8 cells within a few rows of the morphogenetic furrow. Recent results suggest that a second bistable switch, based on mutual antagonism between Sens and Ro, takes over from the Ato/Sens positive-feedback loop to maintain the distinct identities of R8 and R2/5 cells (Pepple et al., 2008). Experiments with a *sens* transcriptional reporter imply that Ro directly represses *sens* expression, whereas genetic results imply that the presence of Ro is necessary to prevent *sens* from being expressed in R2/5 cells (Pepple et al., 2008). Conversely, Sens is sufficient to repress *ro* in R2/5 cells and necessary to prevent *ro* expression in R8 cells, although it is not yet known whether transcriptional repression of *ro* by Sens is direct (Frankfort et al., 2001; Frankfort and Mardon, 2004).

Additional work will be needed to understand the interplay between bistable fate choices and tissue-scale patterning and to evaluate to what extent the Ato/Sens and Ro/Sens positive-feedback loops each contribute to bistability. Confronting such questions will require advances in the ability to generate quantitative, time-resolved data, coupled with a continuing search for mathematical frameworks that usefully organize these data.

R3 versus R4: an intercellular switch

Adult ommatidia are chiral structures, yet developing ommatidia are at first bilaterally symmetric. The choice between photoreceptors R3 and R4 supplies the initial directional cue that breaks ommatidial symmetry. Coordinated bistable fate choice in the R3/R4 pair relies upon the action of two coupled intercellular positive-feedback loops involving juxtacrine signaling through the Notch/Delta and Frizzled/planar cell polarity (Fz/PCP) pathways (Fig. 4). Both pathways are thought to generate positive feedback by combining intracellular cross-antagonism with intercellular cross-activation between pairs of factors.

As described above, Notch-mediated lateral inhibition is used to specify R8 cells in a stochastic, but spatially regular, manner. By contrast, Notch-mediated lateral inhibition between the R3 and R4 precursors generates a two-cell bistable switch that responds deterministically to an external signaling gradient (Fig. 4). This switch involves: (1) cell-autonomous transcriptional repression of *Delta* ligand by Notch signaling; and (2) non-cell-autonomous activation of Notch signaling by Delta ligand on the surface of the adjacent cell (Cooper and Bray, 1999; Fanto and Mlodzik, 1999; Sprinzak et al., 2010). Together, these interactions generate positive feedback that amplifies differences in Delta/Notch signaling between the R3 and R4 precursors. The end result is a system with two stable states in which the presumptive R3 cell has high Delta expression and low Notch pathway activation and the R4 precursor has high Notch pathway activation and low Delta expression.

Signaling through the receptor Fz appears to provide the initial bias that coordinates the direction of the R3 versus R4 decision by inducing the expression of the Notch ligand Delta (Zheng et al., 1995; Cooper and Bray, 1999; Fanto and Mlodzik, 1999; Yang et al., 2002). An apparent gradient of Fz activity, which is high at the equator (the dorsoventral boundary of the eye disc; see Fig. 1A) and decreases towards the periphery, results in slightly higher Delta expression in the precursor cell closer to the equator. This initial bias is amplified by the Delta/Notch feedback loop described above, and results in the cell nearest to the equator becoming the R3 photoreceptor and the cell further from the equator becoming R4 (Cooper and Bray, 1999; Fanto and Mlodzik, 1999).

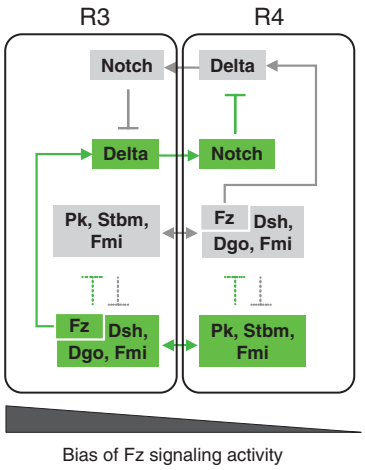

Fig. 4. An intercellular switch that distinguishes R3 from R4. Delta/Notch signaling and possibly also planar cell polarity (PCP) signaling are involved in generating a bistable switch that distinguishes between photoreceptors R3 and R4 in the developing *Drosophila* eye imaginal disc. Notch signaling promotes bistability via intracellular cross-antagonism and intercellular cross-activation between Notch and its ligand Delta. Frizzled (Fz) signaling preferentially activates Delta in the cell nearer the equator, causing it to become R3 while inducing its neighbor to become R4. Heterotypic association of different PCP complexes across the interface between the two cells, together with putative intracellular cross-antagonism in the formation of the two complexes, may also generate bistability by exploiting the same basic principle used by the Delta/Notch switch. In addition to activating Delta expression, Fz serves as a core component of the PCP signaling pathway, although it remains unclear how these two functions of Fz are related. For key, see Fig. 3 legend.

In addition to this Delta/Notch switch, the R3 versus R4 decision is influenced by signaling through the PCP pathway. Although the detailed mechanisms of PCP signaling remain incompletely understood and controversial (Lawrence et al., 2007; Lawrence et al., 2008), one suggested mechanism involves bistability in the formation of alternate signaling complexes at the interface between R3 and R4 (for reviews, see Strutt and Strutt, 2009; Klein and Mlodzik, 2005). A complex containing Fz, Dishevelled (Dsh) and Diego (Dgo) becomes enriched at the R3 side of the R3-R4 interface, while a complex containing Prickle (Pk) and Strabismus (Stbm; Van Gogh – FlyBase) becomes enriched at the R4 side (Strutt et al., 2002; Jenny et al., 2003; Das et al., 2004). Fz- and Stbm-containing complexes may promote the formation of the 'opposite' complex in the adjacent cell via heterotypic interactions across cell-cell junctions (Chen et al., 2008; Strutt and Strutt, 2008). At the same time, intracellular mutual antagonism in the formation of these two complexes has been proposed, perhaps mediated in part by competition between Fz and Stbm to bind to their common co-factor Flamingo (Fmi; Starry night – FlyBase) (Das et al., 2002; Jenny et al., 2003; Strutt and Strutt, 2008; Strutt

and Strutt, 2009). Thus, similar to the two-cell Delta/Notch switch, the combination of intercellular cross-activation and intracellular cross-antagonism in the PCP pathway may generate a bistable pattern of signaling between a pair of cells (Fig. 4) (Axelrod, 2009). How the decisions of the Delta/Notch and PCP switches are coupled remains an open question. In particular, it is unclear whether the function of Fz as a regulator of the Delta/Notch switch is related to its role in PCP signaling.

Computational models exploring two competing hypotheses of PCP signaling in the wing and of coupled Delta/Notch and PCP signaling in R3/4 have been reported (Amonlirdviman et al., 2005; Le Garrec et al., 2006; Le Garrec and Kerszberg, 2008). It is likely that such models, alongside experiments designed to elucidate basic mechanisms, will be helpful for understanding how the Delta/Notch and PCP pathways cooperate to drive cell-fate choice.

The Yan network: a general switch for differentiation

Above, we discussed two cases in which extracellular signals drive a bistable switch towards one outcome or another to produce specific cell fates. Studies of the Yan network, which comprises a conserved set of factors downstream of receptor tyrosine kinase (RTK) signaling (Fig. 5), suggest that this network acts as a bistable switch that maintains the more general distinction between differentiated cells and undifferentiated precursors in the *Drosophila* eye.

The Yan protein (Anterior open – FlyBase) is an Ets family transcriptional repressor that is initially present in all undifferentiated cells at, and posterior to, the morphogenetic furrow (Lai and Rubin, 1992). In response to RTK signaling, Yan is inactivated by phosphorylation by mitogen-activated protein kinase (Mapk; Rolled – FlyBase) (O'Neill et al., 1994; Rebay and Rubin, 1995). Mapk concomitantly phosphorylates and activates PntP2, the P2 isoform of another Ets family transcription factor, Pointed, which binds enhancers vacated by Yan to activate RTK target genes (Brunner et al., 1994; O'Neill et al., 1994).

In addition to being downregulated by Mapk signaling, Yan activity is inhibited in at least three other ways: (1) it is antagonized by the constitutively active P1 isoform of Pnt (PntP1) at a transcriptional level (Rohrbaugh et al., 2002); (2) its translation is repressed by the microRNA miR-7 (Li and Carthew, 2005; Li et al., 2009); and (3) it is inactivated post-translationally by direct interaction with the protein Mae (Edl – FlyBase) (Baker et al., 2001; Tootle et al., 2003; Qiao et al., 2004). In turn, Yan transcriptionally represses the expression of both *mae* and *miR-7*, whereas both are induced by RTK signaling through Pnt (Vivekanand et al., 2004; Li and Carthew, 2005; Li et al., 2009). Expression of *pntP1* is also upregulated by RTK signaling (Gabay et al., 1996), suggesting that it too is a transcriptional target of Yan and Pnt.

The mutual antagonism between Yan and this set of co-regulated factors suggests that the overall network might be bistable (Fig. 5). Although such bistability remains to be demonstrated experimentally, having a bistable switch downstream of Mapk would be ideal for generating all-or-none responsiveness to RTK signaling. Once a cell received an RTK signal of sufficient strength, it would be driven to differentiate by being flipped to a self-sustaining low-Yan state. Under conditions of low-level RTK signaling, sustained Yan activity would prevent precursor cells from differentiating prematurely.

A mathematical model of the Yan network switch

Although the above qualitative argument suggests that the Yan network might exhibit switch-like behavior, it would be difficult using qualitative intuition alone to predict the detailed dynamics of the three coupled transcriptional, translational and post-translational positive-feedback loops or to understand the functional relevance of the network's complex topology. Mathematical models provide a complementary tool for exploring the behavior of such networks and for studying the importance of specific interactions for their overall dynamics. Here, we present a novel mathematical representation of the Yan network to illustrate how the quantitative response of this network to signaling can be simulated computationally.

Our model contains the core components listed in Box 1 plus a variable RTK (Erk/Mapk) input. The rate of change in the concentration of each component is described by the equations listed in Box 1 (see also Box 2 and Table 1), and each indicated interaction is represented by a term in these equations. Different patterns of gene expression emerge from the same equations, depending on the initial concentrations of molecules. In the model, switching from a high-Yan, low-PntP1 state to a high-PntP1, low-Yan state can be triggered by a pulse of RTK signal. Conversely, the model predicts that a transient pulse of Yan overexpression should be able to flip the switch from a low-Yan state back to its original high-Yan, low-PntP1 state, barring irreversible downstream events.

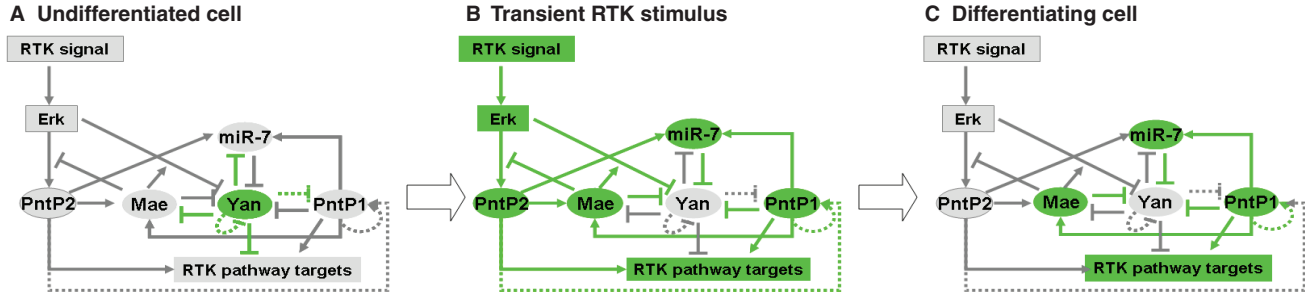

Fig. 5. The Yan network switch. Putative role of the Yan network as a bistable switch that regulates differentiation in the eye imaginal disc. (**A**) The Yan network consists of a group of regulators downstream of RTK signaling. The 'core' of the network comprises the transcriptional repressor Yan and three other factors (PntP1, Mae and miR-7), with which Yan is mutually antagonistic. In the absence of RTK signaling, the network exists in a high-Yan state, which prevents cells from differentiating prematurely. (**B**) In response to a transient pulse of RTK signal, Mapk phosphorylates and inactivates Yan while inducing its antagonists. (**C**) In our proposed bistable switch model, this transient stimulus induces a sustained transition from a stable high-Yan state to a stable high-PntP1, high-Mae, high-miR-7 state that drives differentiation. For key, see Fig. 3 legend.

Box 1. A model of the Yan network

To model cell-fate choice governed by the Yan network, we translate the interactions in Fig. 5 into the following set of chemical rate equations for the following molecular species: Y, Yan protein; m_Y, *yan* mRNA; P_1 and P_2, Pointed proteins P1 and P2; M, Mae protein; M:Y, Mae-Yan heterodimer; M:P_2, Mae-PntP2 heterodimer; m_{R7}, miR-7; m_Y:m_{R7}, *yan* mRNA–miR-7 complex; E, activated Erk/Mapk; asterisk indicates phosphorylation.

$$\dot{Y} = -\vec{k}_{M:Y}\,MY + \overleftarrow{k}_{M:Y}\,M:Y + k_Y^t m_Y - d_Y Y$$

$$\dot{m}_Y = H_{m_Y}(P_1, P_2^*, Y) - \vec{k}_{m_{R7}}\,m_{R7}m_Y + \overleftarrow{k}_{m_{R7}}\,m_Y:m_{R7} - d_{m_Y}m_Y$$

$$\dot{Y}^* = -\vec{k}_{M:Y^*}\,MY^* + \overleftarrow{k}_{M:Y^*}\,M:Y^* - d_{Y^*}Y^*$$

$$\dot{P}_1 = G_{P_1}(Y)F_{P_1}(P_1, P_2^*) - d_{P_1}P_1$$

$$\dot{P}_2 = e_{P_2} - \frac{\alpha_{P_2^*}EP_2}{P_2 + K_{P_2^*}} - \vec{k}_{MP_2}\,MP_2 + \overleftarrow{k}_{MP_2}\,M:P_2 - d_{P_2}P_2$$

$$\dot{P}_2^* = \frac{\alpha_{P_2^*}EP_2}{P_2 + K_{P_2^*}} - d_{P_2^*}P_2^*$$

$$\dot{M} = G_M(Y)F_M(P_1, P_2^*) - \vec{k}_{MP_2}\,MP_2 + \overleftarrow{k}_{MP_2}\,M:P_2 - \vec{k}_{M:Y}\,MY - \vec{k}_{M:Y^*}\,MY^* + \overleftarrow{k}_{M:Y^*}\,M:Y^* + \overleftarrow{k}_{M:Y}\,M:Y - d_M M$$

$$\dot{M}:Y = -\frac{\alpha_{Y^*}EM:Y}{M:Y + K_{Y^*}} + \vec{k}_{M:Y}\,MY - \overleftarrow{k}_{M:Y}\,M:Y - d_{M:Y}M:Y$$

$$\dot{M}:Y^* = \frac{\alpha_{Y^*}EM:Y}{M:Y + K_{Y^*}} + \vec{k}_{M:Y^*}\,MY^* - \overleftarrow{k}_{M:Y^*}\,M:Y^* - d_{M:Y^*}M:Y^*$$

$$\dot{M}:P_2 = \vec{k}_{MP_2}\,MP_2 - \overleftarrow{k}_{MP_2}\,M:P_2 - d_{MP_2}M:P_2$$

$$\dot{m}_{R7} = G_{m_{R7}}(Y)F_{m_{R7}}(P_1, P_2^*) - \vec{k}_{m_{R7}}\,m_{R7}m_Y + \overleftarrow{k}_{m_{R7}}\,m_Y:m_{R7} - d_{m_{R7}}m_{R7}$$

$$\dot{m}_Y:m_{R7} = \vec{k}_{m_{R7}}\,m_{R7}m_Y - \overleftarrow{k}_{m_{R7}}\,m_Y:m_{R7} - d_{m_Y:m_{R7}}m_Y:m_{R7}$$

A dot above a species denotes its time derivative (i.e. $\dot{x}=dx/dt$). The parameters are defined in Table 1.

The Hill functions that are employed to describe transcriptional regulation are:

$$F_X(P_1, P_2^*) = \frac{\alpha_X(p_{1X}P_1 + p_{2X}P_2^*)^{n_X}}{k_X^{n_X} + (p_{1X}P_1 + p_{2X}P_2^*)^{n_X}} + e_X$$

$$G_X(Y) = 1 - \frac{Y^{n'_X}}{k_X'^{n'_X} + Y^{n'_X}}$$

$$H_{m_Y}(P_1, P_2^*, Y) = \frac{\alpha_{m_Y}(p_{1m_Y}P_1 + p_{2m_Y}P_2^* + p_{3m_Y}Y)^{n_{m_Y}}}{k_{m_Y}^{n_{m_Y}} + (p_{1m_Y}P_1 + p_{2m_Y}P_2^* + p_{3m_Y}Y)^{n_{m_Y}}} + e_{m_Y}$$

where $\alpha_{m_Y}<0$.

Box. 2. An explanation of our model

- Mae, PntP1, PntP2 and miR-7 production are approximated as one-step processes.
- Yan transcription and translation are modeled separately to represent miR-7-mediated translational repression of Yan.
- Repression of *yan* by miR-7 is modeled by the formation of a binary complex of *yan* mRNA and miR-7, in which *yan* mRNA cannot be translated.
- When complexed with Mae, Yan is assumed to be inactive as a transcriptional repressor and to be more easily phosphorylated by Erk/Mapk.
- Binding reactions are represented using standard second-order rate laws.
- Phosphorylation of PntP2, Yan alone, and Yan within the Yan-Mae heterodimer are assumed to follow Michaelis-Menten kinetics.
- Degradation of each component is assumed to follow first-order kinetics.
- To model the efficient phosphorylation-induced degradation of Yan, the degradation rate constant of phosphorylated Yan was set to be much higher than that of unphosphorylated Yan. It was assumed that phosphorylated Yan would have to dissociate from Mae before being degraded. This dissociation was made to be very rapid (i.e. $\overleftarrow{k}_{M:Y^*} >> \overleftarrow{k}_{M:Y}$).

Given an incomplete knowledge of the details of the system, it is important to assess the sensitivity of the model behavior to the choice of parameters (e.g. protein production rates, degradation rates, and parameters describing gene regulation). Often, certain ratios of parameters are constrained by limited data, even though their individual values are not (Gutenkunst et al., 2007). Although feasible for simpler models, the systematic exploration of the space of parameter choices becomes more difficult as models become more elaborate. One approach is to test many different sets of parameters within a given range and then to determine which sets are consistent with a given behavior (Ben-Zvi et al., 2008; Pennington and Lubensky, 2010). A simpler option is to fix most of the parameters at values that yield reasonable behavior and to vary the remainder systematically. The example shown in Fig. 6 illustrates the sensitivity of the model to the maximal rate of Yan production. The PntP1 and Yan concentrations at all stable states are plotted as a function of the maximal rate of Yan production. Remarkably, the network remains bistable even while the value of this parameter spans nearly three orders of magnitude (Fig. 6A). If the maximal Yan production rate becomes too low, the system has only one stable state (high PntP1). If the Yan production rate becomes too high, the system is also monostable (with high Yan). These effects derive from shifts in the balance of production and degradation rates, like those illustrated in Fig. 2B.

It might be possible to sample these three different bistable and monostable regimes experimentally. The wild-type Yan network is thought to be bistable, yet the model predicts that it should be possible to enter a monostable regime by decreasing the production rate of Yan. Our model suggests that the differentiation of ectopic photoreceptors in *yan* loss-of-function mutants (Lai and Rubin, 1992) might reflect not just sensitization of these cells to RTK signaling, but also a more fundamental conversion of the Yan network from a bistable to a monostable state. In cells in which Yan production is sufficiently reduced, the model predicts that the low-Yan, high-PntP1 state will become the only option, leading cells to differentiate regardless of the level of RTK signaling they receive. Consistent with this idea, reducing RTK signaling through mutation of the Sevenless (Sev) RTK fails to suppress the gain-of-photoreceptor-R7 phenotype in the yan^1 hypomorphic mutant (Lai and Rubin, 1992). Similar epistasis experiments using alleles that abolish all RTK signaling will be needed to test this idea more rigorously.

Experimentally, entering the second, high-Yan monostable regime appears to require very high levels of wild-type *yan* transgene expression (I.R., unpublished data). However, moderate overexpression of Yan^{Act}, a constitutively active, non-phosphorylatable mutant of Yan that escapes RTK signal-mediated downregulation, effectively blocks photoreceptor differentiation in the *Drosophila* eye (Rebay and Rubin, 1995). To explore how constitutive expression of Yan^{Act} might influence network behavior, we introduced a Yan^{Act}-expressing transgene into the model as a second, non-phosphorylatable Yan species that is produced at a constant rate. When the yan^{Act} mRNA production rate is increased above a certain threshold, the system switches from being bistable to monostable (Fig. 6B). The conventional view is that Yan^{Act} blocks photoreceptor differentiation by repressing genes that would

Table 1. A summary of rate parameter notation

Description of parameter	Notation
Weight of P_1 in activating X	p_{1X}
Weight of P_2^* in activating X	p_{2X}
Weight of Y in activating X	p_{3X}
Activator binding constant for X	k_X
X synthesis rate without activators	e_X
Maximum X production rate	α_x
Hill coefficient of activation	n_x
Repressor binding constant for X	k'_X
Hill coefficient of repression	n'_X
Degradation rate constant of X	d_X
Association rate constant of complex X	$\bar{k}_X$
Dissociation rate constant of complex X	$\hat{k}_X$
k_{cat} for phosphorylation of X	α_{X*}
K_m for phosphorylation of X	K_{X*}

normally be activated by RTK signaling (Rebay and Rubin, 1995). Our model agrees and suggests, moreover, that expression of Yan^{Act} might destroy the essential bistability of the Yan network by destabilizing the high-PntP1 attractor. When Yan^{Act} is expressed above some critical threshold, our model predicts that no level of RTK signal will ever be able to induce photoreceptor differentiation (Fig. 6B). Consistent with this prediction, RTK pathway hyperactivation is unable to modify the phenotype of yan^{S2382}, a gain-of-function allele that partially phenocopies Yan^{Act} (Rebay and Rubin, 1995; Karim et al., 1996). Further experiments will be needed to verify that expression of constitutively active versions of Yan above a specific threshold is able to convert the network from bistable to monostable.

Our model of the Yan network does not yet take into account certain important features of the system, including regulated self-association and localization of Yan, phosphorylation of Yan at multiple sites, and binding of multiple miR-7 molecules to the 3′ UTR of the *yan* mRNA (Rebay and Rubin, 1995; Tootle et al., 2003; Qiao et al., 2004; Li and Carthew, 2005; Zhang et al., 2010). It should be relatively straightforward to include these features in subsequent models. Additional quantitative experiments will be needed to provide reasonable estimates of parameters within the model. Advanced genetic tools should allow specific regulatory links in this network to be specifically ablated, such as the interaction of Yan with Mae, the repression of *yan* mRNA by miR-7, and the negative regulation of *yan* by PntP1. Data on precisely mutated networks will provide additional constraints that the model must satisfy, narrowing down the space of theoretically possible parameter choices. In parallel, it should be possible to estimate certain parameters directly using transgenes expressing fluorescently labeled Yan and PntP1 and transcriptional reporters for the various genes in the network. Inconsistencies between predicted and measured quantities would prompt revisions of the model, thereby advancing our mechanistic understanding of this network.

Coupling bistable switches to generate multistable switches

Above, we have discussed several instances in which bistable switches are thought to mediate specific binary cell-fate choices. Ultimately, such bistable motifs must function as components of larger, more-complex networks that guide the specification of each distinct cell type within a multicellular organism. A longstanding idea, which has recently received experimental support, is that cell fates correspond to high-dimensional attractors in the dynamics of these multistable networks (Waddington, 1957; Kauffman, 1969;

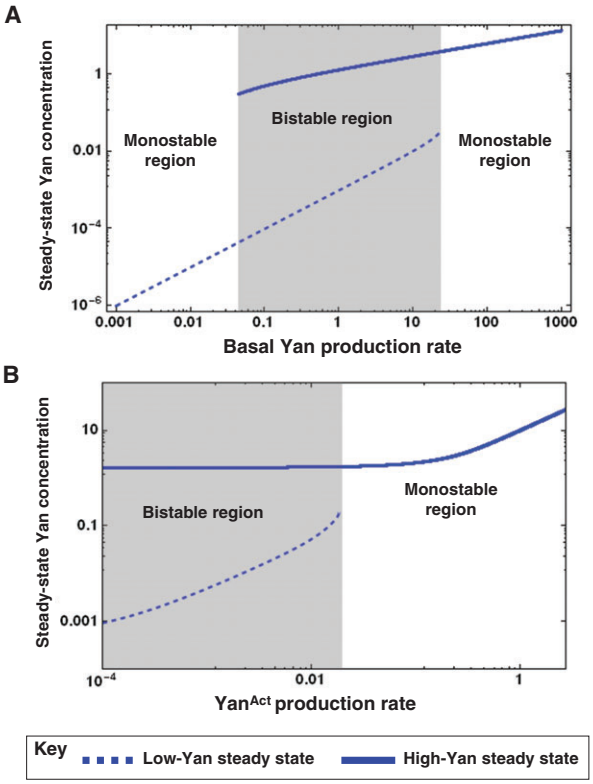

Fig. 6. Sensitivity of the Yan network model to specific parameter choices. Our model of the Yan network demonstrates how changing specific parameters can influence whether the network is monostable or bistable (for more on this model, see Simulation 2 and Tables S1-S4 in the supplementary data for parameter choices used in our simulations of the model). (**A**) Changing a single parameter, i.e. the maximal production rate of Yan, while keeping other parameters constant, can change the number of stable states available to the network. Levels of Yan at different stable states are shown as a function of the maximal Yan production rate (plotted on a logarithmic scale). Two possible stable states (indicated by solid and dashed curves) coexist in the bistable region (gray), whereas only one solution exists in the monostable regions. Bistability of the network is lost when the basal production rate of Yan is tuned to be either too high or too low. (**B**) A similar diagram for the model that includes Yan^{Act}, the non-phosphorylatable constitutive repressor mutant of Yan. Possible steady-state levels of total Yan (endogenous Yan + Yan^{Act}) are plotted versus the logarithm of the production rate of Yan^{Act} (the variable parameter). The system begins in a bistable state (shaded), but bistability is destroyed by expressing a sufficient amount of Yan^{Act}, which reduces the number of stable solutions from two to one.

Huang et al., 2005; Chang et al., 2006; Chang et al., 2008; Bar-Yam et al., 2009; Huang, 2009). In this section, we discuss two previously proposed strategies by which multistable networks can be built from simpler bistable modules (Cinquin and Demongeot, 2002); we refer to these as ‘hierarchical’ and ‘horizontal’. We then present a new hypothesis of cell-fate choice in the R7 equivalence group that employs and illustrates both strategies.

Hierarchical combination of bistable switches

A multistable network can in principle be built from a series of bistable switches linked hierarchically in a binary decision tree (Fig. 7A), with the activity of downstream switches made contingent on the decisions made by upstream switches (Cinquin and Demongeot, 2002; Foster et al., 2009; Wang et al., 2009;

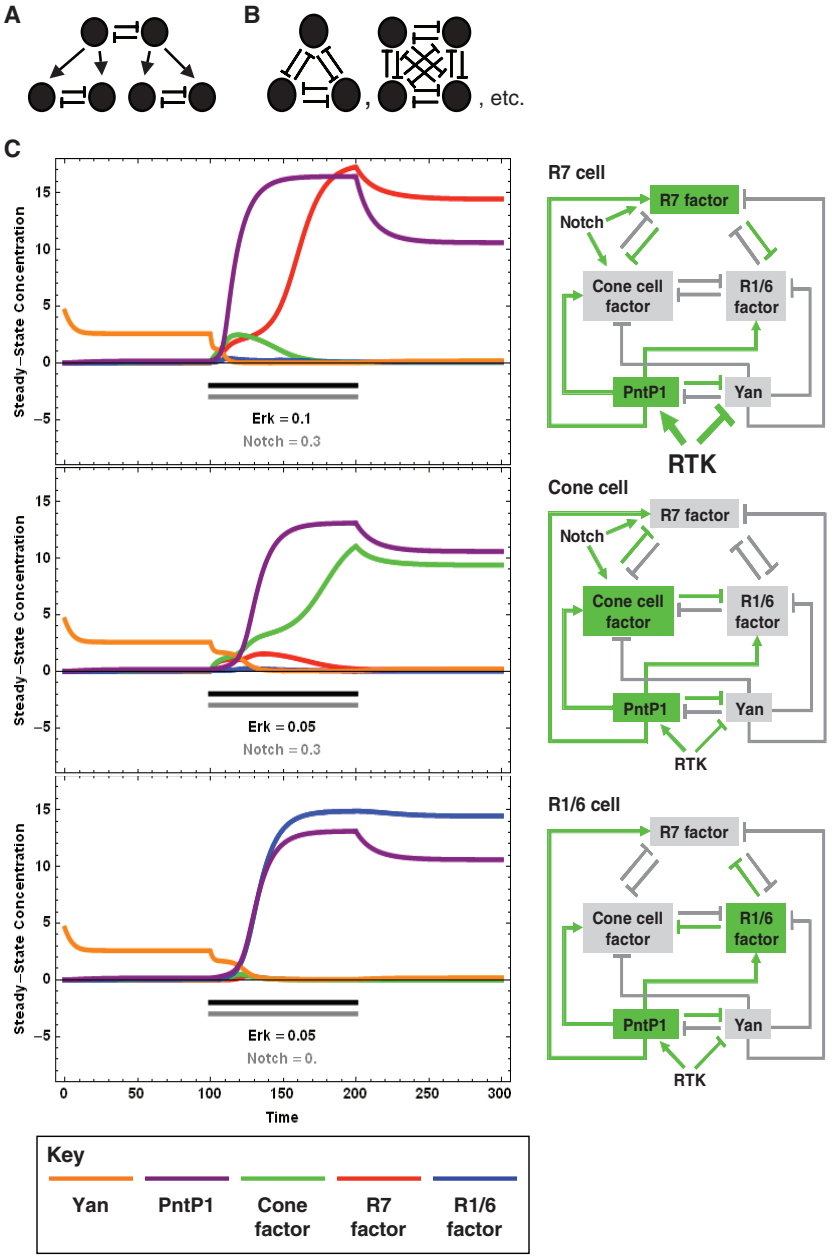

Fig. 7. Schemes for coupling bistable switches into multistable networks. The 'attractive landscape' hypothesis of cell-fate choice (Waddington, 1957; Kauffman, 1969; Huang, 2009) proposes that different cell types correspond to distinct attractors in the dynamics of multistable genetic and signaling networks. Two schemes are illustrated by which multistable networks can be built from simpler bistable components and the output of a mathematical model that embodies both strategies is presented. (**A**) Hierarchical activation by upstream switches of increasingly fate-specific downstream switches gives rise to a tree of branching fate decisions (Cinquin and Demongeot, 2002; Foster et al., 2009; Wang et al., 2009; Artyomov et al., 2010). Here, and in B, circles represent idealized 'factors' that regulate cell-fate choice. (**B**) Horizontal coupling of switches into a network of mutual antagonists may provide multipotent progenitors with simultaneous access to several mutually exclusive fates. (**C**) Output of the multiple bistable switch model for fate choice in the *Drosophila* eye imaginal disc R7 equivalence group, demonstrating how different combinations of transient RTK and Notch signals can flip the switch in the direction of one of the three cell-fate-specific factors. (Left) Plots show results from numerical simulations of our mathematical model in response to different combinations of RTK and Notch signals. The period during which the signals were transiently applied is indicated by black (RTK) and gray (Notch) horizontal lines. (Right) The components that are active (green) and inactive (gray) at the end of each simulation. When stimulated with RTK signal below a critical threshold, the switch returns to its initial high-Yan state (not shown). For more on this model, see Simulation 1 in the supplementary material.

Artyomov et al., 2010). Experimentally observed cell-fate lineages can be considered branches along this decision tree network. Among the switches described above, an example of hierarchical linkage is found in the initial decision between the R2/5 and R8 fates, followed by the subsequent specification of pale and yellow subtypes of R8. In this case, the subtype specification switch involving mutually antagonistic Wts and Melt expression only becomes active if a cell has previously decided to adopt an R8 fate. Mechanistically, how such information is transmitted remains an open question.

Horizontal combination of bistable switches

Bistable switches may also be joined 'horizontally' (or 'simultaneously') by the participation of each factor in multiple switches (Cinquin and Demongeot, 2002; Cinquin and Demongeot, 2005). A simple example of this category is what we term a tristable triad, which is a network with three factors in which each factor represses the other two (Fig. 7B). Given appropriate quantitative parameters (see below), such a network can in principle generate three stable states in which one of the three factors is highly expressed while the other two factors are repressed. Tristable triads have previously been implicated in the specification of *Drosophila* muscle/heart progenitors (Jagla et al., 2002) and have been proposed as the basis for a synthetic tristable switch (Lohmueller et al., 2007). Horizontal coupling of bistable switches could probably be extended to generate multistable switches with an arbitrary number of factors, with the number of required negative regulatory links given by N(N-1), where N is the number of factors/stable states. We note that horizontally coupled multistable motifs of this form can also substitute for bistable motifs in the hierarchical scheme described in Fig. 7A, producing a decision tree in which some decisions involve more than two options (see below for an example).

A model of coupled bistable switches in fate choice in the R7 equivalence group

In this section, we propose a multistable network model of a cell-fate decision that invokes the ideas discussed above. R7, R1/6 and cone cells differentiate from initially tripotent cells in an 'R7 equivalence group' in response to different doses of Notch and RTK signaling (Table 2). It is possible to interconvert these three cell types by changing the levels of the two signals that they receive (Hafen et al., 1987; Freeman, 1996; Cooper and Bray, 2000). For instance, reducing RTK signaling in a presumptive R7 cell converts it to a cone cell (Tomlinson and Ready, 1987). Conversely, increasing RTK signaling causes cone cell precursors to turn into ectopic R7 cells (Fortini et al., 1992). Although this system has been extensively studied, how the genetic networks within each cell respond to quantitative differences in signaling to distinguish these three cell fates is not yet understood.

Below, we consider one possible model in which a multistable network of coupled bistable switches responds to different patterns of RTK and Notch signaling to specify the R1/6, R7 and cone cell fates. In our simplified mathematical model of this network (Box 3), three regulatory factors that are specific to R1/6, R7 and cone cells reinforce their own expression while repressing the expression of the two alternate factors (Fig. 7C). Reasonable candidates for these factors include BarH1 and Seven-up (Svp) for R1/6 (Mlodzik et al., 1990; Higashijima et al., 1992; Hiromi et al., 1993; Hayashi et al., 1998; Miller et al., 2008); Spalt major (Salm), Phyllopod (Phyl), Seven in absentia (Sina) and Prospero (Pros) for R7 (Li et al., 1997; Xu et al., 2000; Cook et al., 2003; Domingos et al., 2004; Hayashi et al., 2008); and Pax2 (Shaven – FlyBase), Tramtrack (Ttk) and Cut for cone cells (Canon and Banerjee, 2003; Shi and Noll, 2009). Each relationship between cell-fate determinants in the model can be thought of as a separate bistable switch. These three switches are horizontally coupled to form a tristable triad, the stable states of which correspond to the expression of one of the three factors and the repression of the other two.

Also built into the model are inputs from the Notch and RTK pathways that bias the compound switch to choose one fate over the other two. The RTK input is communicated through the Yan network switch, which has a hierarchical relationship to the downstream three-factor tristable switch. For the downstream network to be active, and for differentiation to occur at all, the Yan network must first be flipped from a high-Yan to a high-PntP1 state.

Notch and RTK signaling can flip the R1/6-R7, R7-cone and R1/6-cone switches in our model only if they differentially regulate the three fate-specific factors. Several pieces of experimental evidence support this idea. Notch directly or indirectly represses the R1/6-specific factors Svp and BarHI (Cooper and Bray, 2000; Hayashi et al., 2008). By contrast, the R7 and cone cell determinants Pros and Pax2 are induced by combined Notch and RTK signals, although with differing thresholds for activation by the two signals (Flores et al., 2000; Xu et al., 2000; Swanson et al., 2010). Full induction of Pros in R7 cells requires high levels of RTK pathway activity, whereas full induction of the cone cell factor Pax2 requires high levels of Notch activity. These relationships provide exactly the sort of biased activation of R7- and cone-specific genes required by our model.

Fig. 7C shows simulations of our model in which an initially high-Yan (undifferentiated) cell is stimulated with different combinations of Notch and RTK signals (see Simulation 1). Stimulation by RTK signaling in all cases flips the Yan network switch to a high-PntP1 state, enabling downstream fate-specific genes to be turned on. When a cell only receives an RTK signal, R1/6-specific factors are induced, whereas Notch-dependent R7 and cone cell factors are not. In response to both Notch and RTK signaling, the balance of the two signals guides the cell to an R7 or cone fate, with higher RTK signaling favoring R7 and higher Notch signaling favoring the cone cell fate (a detailed phase diagram of the response of this model to RTK and Notch signals is supplied in Simulation 1 in the supplementary material). Because Boss and Delta ligands (which activate RTK and Notch signaling, respectively) are restricted to the surfaces of neighboring cells, different combinations of these two signals are accessed by different arrangements of cells in the ommatidium, directly coupling differentiation and spatial patterning.

Box 3. A hypothesis for cell-fate choice in the R7 equivalence group

The equations in our model of R7 equivalence group fate choice are:

$$\dot{A} = \frac{1}{B^2+1}\left[\frac{1.5P^3}{(0.579C^3+1)(P^3+8)(Y^2+1)} + \frac{Notch^2}{Notch^2+0.25}\right] - 0.1\,A$$

$$\dot{B} = \frac{1}{A^2+1}\left[\frac{P^2}{(1.953C^3+1)(P^2+1)(Y^2+1)} + \frac{Notch^2}{Notch^2+0.25}\right] - 0.1\,B$$

$$\dot{C} = \frac{1.5P^2}{(A^2+1)(B^3+1)(P^2+1)(Y^2+1)} - 0.1\,C$$

$$\dot{P} = \frac{1}{Y^2+1}\left(\frac{E^2}{E^2+0.01}+1\right)\left(\frac{P^2}{P^2+1}+0.1\right) - 0.1\,P$$

$$\dot{Y} = \frac{2}{(P^2+1)(Y^2+1)} - 0.1\left(\frac{10E^2}{E^2+0.01}+1\right)Y,$$

where A represents the R7 factor, B represents the cone factor, C represents the R1/6 factor, Y and P represent Yan and PntP1, and E represents Erk/Mapk.

The functions describing activation of the R1/6, R7 and cone factors have been chosen such that they are induced most strongly in the presence of RTK signaling alone, moderate Notch signaling and strong RTK signaling, or moderate RTK signaling and strong Notch signaling, respectively. Although these differences in regulation may be quantitatively subtle, the mutual antagonism between each pair of factors amplifies even small differences to drive a cell robustly towards one of the three distinct fates. The driving force for this robust fate choice arises mathematically from the inherent instability of intermediate states where more than one factor is expressed at once.

Table 2. Cell-fate choice in the R7 equivalence group in response to different levels of RTK and Notch signaling

RTK signal	Notch signal	Resulting fate	References
+ (Egfr)	–	R1/6	(Freeman, 1996; Cooper and Bray, 2000; Hayashi et al., 2008)
+ (Egfr)	++	Cone	(Flores et al., 2000; Pickup et al., 2009)
++ (Egfr + Sevenless)	+	R7	(Hafen et al., 1987; Xu et al., 2000; Cooper and Bray, 2000; Tomlinson and Struhl, 2001)

Although the details of the R7 equivalence group network will undoubtedly be more complex than the simple model we have proposed here, it will be interesting to determine whether the overall network can indeed be broken down into a combination of bistable switch-like components. Our model predicts that it will be particularly productive to search for direct transcriptional regulatory links between master regulators that allow cross-antagonism to occur between alternate R1/6, R7 and cone cell fates. It might turn out that even a simple coarse-grained model, like the one we have proposed, is useful for understanding the dynamics of key master regulators during normal development or in response to externally applied signaling perturbations. Advances in quantifying signaling inputs and gene-regulatory responses experimentally might eventually make it possible to construct fate maps showing the probability of choosing different fates as a function of inputs (see Simulation 1 in the supplementary material). Mapping the responses of single cells to different combinations of signals would provide a powerful means of visualizing the regulatory landscape that governs cell-fate choice, and would provide an excellent means of calibrating and testing future models.

Conclusions

Although bistable genetic switches provide a natural mechanism for distinguishing cell types, much additional work, both experimental and computational, will be needed to understand the relative contributions of multiple positive feedbacks to the generation of bistable cell-fate switches, how these individual switches are wired together into multistable networks, and how such networks mediate cell-fate decisions.

From a broader perspective, bistable and multistable networks must be integrated in space and time within the more complex 'four-dimensional' networks that encode the full developmental program. Which global mechanisms coordinate this program is not yet clear, although the establishment of distinct chromatin states and perhaps even multistability at the level of chromatin modifications or DNA methylation have been proposed as important mechanisms underlying the spatiotemporal coordination of cell fate (Dodd et al., 2007; Mikkelsen et al., 2007; Meissner et al., 2008). We argue that the *Drosophila* eye, with its proven track record as a system for elucidating novel and conserved mechanisms of cell-fate choice, provides a uniquely high-throughput platform for studying developmental pattern formation, and one that is amenable to merging quantitative mathematical modeling with in vivo analysis of signaling dynamics.

Given the clear importance of temporal coordination of developmental programs, experimental techniques that allow us to observe the dynamics of cell-fate choice directly, rather than relying on static snapshots of fixed tissues, will be crucial to developing more accurate and predictive mathematical representations. This will require the manipulation of biological systems in quantitatively precise ways and the collection of quantitative data. Ultimately, one would like to be able to measure network responses in vivo in a developing tissue at single-cell, and even single-molecule, resolution. Although much progress has been made towards achieving these goals in single-celled organisms (Cai et al., 2006; Elf et al., 2007; Choi et al., 2008), extending these approaches to more complex tissues remains a huge challenge.

Towards this goal, efforts to culture eye imaginal discs in vitro, in such a way that allows their continued development to be observed, must be a top priority. In this context, microfluidic systems might provide a means of maintaining the viability of the tissue during continuous observation, while allowing temporally and spatially precise perturbations to be applied (Lucchetta et al., 2005; Lucchetta et al., 2009). Alternatively, advances in multi-photon fluorescence microscopy might eventually permit direct in vivo observations in intact larvae (Huisken and Stainier, 2009; Vinegoni et al., 2009).

A requirement for using live-imaging techniques to investigate signaling dynamics during cell-fate specification is of course to have the key network components tagged with fluorescent markers, such that their expression and activity can be followed dynamically in space and time both in wild-type animals and in those in which specific genetic perturbations have been introduced. Recombineering technology, coupled with ΦC31 integrase-based transformation, permits the manipulation of large genomic sequences and will thus be key to generating the necessary tools and reporters (Venken et al., 2006; Bateman and Wu, 2008). Once appropriate fluorescent readouts of network and cell-fate states are in hand, the extensive genetic tools available in *Drosophila* will allow the introduction of temporally and spatially precise perturbations and the quantitative assessment of their consequences.

Together, such dynamic observations should provide direct evidence for the existence of specific attractor states in genetic networks. For instance, one could test whether artificially induced intermediate patterns of gene expression are inherently unstable, relaxing towards one of two options. Additionally, one might test whether transient perturbations can switch cells between discrete states of gene expression, and whether the gene expression patterns of such 'transdifferentiated' cells always become identical to those of cells that have differentiated via the normal developmental route. The effects of targeted genetic perturbations, when analyzed in conjunction with mathematical simulations, will provide new insights into how specific regulatory interactions within networks contribute to generating these switch-like behaviors.

In conclusion, the power of *Drosophila* genetics has yielded incredible insight into the elaborate sequence of cell-fate choices that pattern each ommatidium, and has provided tantalizing hints about the sorts of switch-like network behaviors that drive them. An expanding range of genetic tools, combined with increasingly quantitative methods for perturbing, measuring, and modeling the system, will undoubtedly provide insights into the conserved strategies and network motifs that cells use to make specific fate choices in the *Drosophila* eye and beyond.

Acknowledgements

We thank our colleagues in the A.R.D. and I.R. laboratories for stimulating discussions and Rich Carthew for helpful comments on the manuscript. The collaboration between I.R. and A.R.D. was supported by the NIH. Additional support to T.G.W.G. was provided by the NIH Roadmap Physical and Chemical Biology Training Program, to S.M.A.T. by the International Human Frontier Science Program Organization (HFSP), and to I.R. by the NIH. Deposited in PMC for release after 12 months.

Competing interests statement

The authors declare no competing financial interests.

Supplementary material

Supplementary material for this article is available at
http://dev.biologists.org/lookup/suppl/doi:10.1242/dev.044826/-/DC1

References

Ackers, G. K., Johnson, A. D. and Shea, M. A. (1982). Quantitative model for gene regulation by lambda phage repressor. *Proc. Natl. Acad. Sci. USA* **79**, 1129-1133.

Albeck, J. G., Burke, J. M., Spencer, S. L., Lauffenburger, D. A. and Sorger, P. K. (2008). Modeling a snap-action, variable-delay switch controlling extrinsic cell death. *PLoS Biol.* **6**, 2831-2852.

Amonlirdviman, K., Khare, N. A., Tree, D. R. P., Chen, W.-S., Axelrod, J. D. and Tomlin, C. J. (2005). Mathematical modeling of planar cell polarity to understand domineering nonautonomy. *Science* **307**, 423-426.
Arkin, A., Ross, J. and McAdams, H. H. (1998). Stochastic kinetic analysis of developmental pathway bifurcation in phage lambda-infected Escherichia coli cells. *Genetics* **149**, 1633-1648.
Artyomov, M. N., Meissner, A. and Chakraborty, A. K. (2010). A model for genetic and epigenetic regulatory networks identifies rare pathways for transcription factor induced pluripotency. *PLoS Comput. Biol.* **6**, e1000785.
Axelrod, J. D. (2009). Progress and challenges in understanding planar cell polarity signaling. *Semin. Cell Dev. Biol.* **20**, 964-971.
Baker, D. A., Mille-Baker, B., Wainwright, S. M., Ish-Horowicz, D. and Dibb, N. J. (2001). Mae mediates MAP kinase phosphorylation of Ets transcription factors in Drosophila. *Nature* **411**, 330-334.
Baker, N. E. and Zitron, A. E. (1995). Drosophila eye development: Notch and Delta amplify a neurogenic pattern conferred on the morphogenetic furrow by scabrous. *Mech. Dev.* **49**, 173-189.
Baker, N. E. and Yu, S. Y. (1997). Proneural function of neurogenic genes in the developing Drosophila eye. *Curr. Biol.* **7**, 122-132.
Baker, N. E., Yu, S. and Han, D. (1996). Evolution of proneural atonal expression during distinct regulatory phases in the developing Drosophila eye. *Curr. Biol.* **6**, 1290-1301.
Baonza, A. and Freeman, M. (2001). Notch signalling and the initiation of neural development in the Drosophila eye. *Development* **128**, 3889-3898.
Bar-Yam, Y., Harmon, D. and de Bivort, B. (2009). Systems biology: attractors and democratic dynamics. *Science* **323**, 1016-1017.
Bateman, J. R. and Wu, C. T. (2008). A simple polymerase chain reaction-based method for the construction of recombinase-mediated cassette exchange donor vectors. *Genetics* **180**, 1763-1766.
Becskei, A., Séraphin, B. and Serrano, L. (2001). Positive feedback in eukaryotic gene networks: cell differentiation by graded to binary response conversion. *EMBO J.* **20**, 2528-2535.
Bell, M. L., Earl, J. B. and Britt, S. G. (2007). Two types of Drosophila R7 photoreceptor cells are arranged randomly: a model for stochastic cell-fate determination. *J. Comp. Neurol.* **502**, 75-85.
Ben-Zvi, D., Shilo, B.-Z., Fainsod, A. and Barkai, N. (2008). Scaling of the BMP activation gradient in Xenopus embryos. *Nature* **453**, 1205-1211.
Bintu, L., Buchler, N. E., Garcia, H. G., Gerland, U., Hwa, T., Kondev, J. and Phillips, R. (2005). Transcriptional regulation by the numbers: models. *Curr. Opin. Genet. Dev.* **15**, 116-124.
Birkholz, D. A., Chou, W.-H., Phistry, M. M. and Britt, S. G. (2009). rhomboid mediates specification of blue- and green-sensitive R8 photoreceptor cells in Drosophila. *J. Neurosci.* **29**, 2666-2675.
Brunner, D., Ducker, K., Oellers, N., Hafen, E., Scholz, H. and Klambt, C. (1994). The ETS domain protein pointed-P2 is a target of MAP kinase in the sevenless signal transduction pathway. *Nature* **370**, 386-389.
Cai, L., Friedman, N. and Xie, X. S. (2006). Stochastic protein expression in individual cells at the single molecule level. *Nature* **440**, 358-362.
Canon, J. and Banerjee, U. (2003). In vivo analysis of a developmental circuit for direct transcriptional activation and repression in the same cell by a Runx protein. *Genes Dev.* **17**, 838-843.
Chang, H., Oh, P., Ingber, D. and Huang, S. (2006). Multistable and multistep dynamics in neutrophil differentiation. *BMC Cell Biol.* **7**, 11.
Chang, H. H., Hemberg, M., Barahona, M., Ingber, D. E. and Huang, S. (2008). Transcriptome-wide noise controls lineage choice in mammalian progenitor cells. *Nature* **453**, 544-547.
Chen, W.-S., Antic, D., Matis, M., Logan, C. Y., Povelones, M., Anderson, G. A., Nusse, R. and Axelrod, J. D. (2008). Asymmetric homotypic interactions of the atypical cadherin flamingo mediate intercellular polarity signaling. *Cell* **133**, 1093-1105.
Choi, P. J., Cai, L., Frieda, K. and Xie, X. S. (2008). A stochastic single-molecule event triggers phenotype switching of a bacterial cell. *Science* **322**, 442-446.
Chou, W. H., Hall, K. J., Wilson, D. B., Wideman, C. L., Townson, S. M., Chadwell, L. V. and Britt, S. G. (1996). Identification of a novel Drosophila opsin reveals specific patterning of the R7 and R8 photoreceptor cells. *Neuron* **17**, 1101-1115.
Chou, W. H., Huber, A., Bentrop, J., Schulz, S., Schwab, K., Chadwell, L. V., Paulsen, R. and Britt, S. G. (1999). Patterning of the R7 and R8 photoreceptor cells of Drosophila: evidence for induced and default cell-fate specification. *Development* **126**, 607-616.
Cinquin, O. and Demongeot, J. (2002). Positive and negative feedback: striking a balance between necessary antagonists. *J. Theor. Biol.* **216**, 229-241.
Cinquin, O. and Demongeot, J. (2005). High-dimensional switches and the modelling of cellular differentiation. *J. Theor. Biol.* **233**, 391-411.
Cook, T., Pichaud, F., Sonneville, R., Papatsenko, D. and Desplan, C. (2003). Distinction between color photoreceptor cell fates is controlled by Prospero in Drosophila. *Dev. Cell* **4**, 853-864.
Cooper, M. T. and Bray, S. J. (1999). Frizzled regulation of Notch signalling polarizes cell fate in the Drosophila eye. *Nature* **397**, 526-530.
Cooper, M. T. and Bray, S. J. (2000). R7 photoreceptor specification requires Notch activity. *Curr. Biol.* **10**, 1507-1510.
Das, G., Reynolds-Kenneally, J. and Mlodzik, M. (2002). The atypical cadherin Flamingo links Frizzled and Notch signaling in planar polarity establishment in the Drosophila eye. *Dev. Cell* **2**, 655-666.
Das, G., Jenny, A., Klein, T. J., Eaton, S. and Mlodzik, M. (2004). Diego interacts with Prickle and Strabismus/Van Gogh to localize planar cell polarity complexes. *Development* **131**, 4467-4476.
Dodd, I. B., Micheelsen, M. A., Sneppen, K. and Thon, G. (2007). Theoretical analysis of epigenetic cell memory by nucleosome modification. *Cell* **129**, 813-822.
Dokucu, M. E., Zipursky, S. L. and Cagan, R. L. (1996). Atonal, rough and the resolution of proneural clusters in the developing Drosophila retina. *Development* **122**, 4139-4147.
Domingos, P. M., Brown, S., Barrio, R., Ratnakumar, K., Frankfort, B. J., Mardon, G., Steller, H. and Mollereau, B. (2004). Regulation of R7 and R8 differentiation by the spalt genes. *Dev. Biol.* **273**, 121-133.
Dubnau, D. and Losick, R. (2006). Bistability in bacteria. *Mol. Microbiol.* **61**, 564-572.
Edgar, B. A., Odell, G. M. and Schubiger, G. (1989). A genetic switch, based on negative regulation, sharpens stripes in greater embryos. *Dev. Genet.* **10**, 124-142.
Elf, J., Li, G.-W. and Xie, X. S. (2007). Probing transcription factor dynamics at the single-molecule level in a living cell. *Science* **316**, 1191-1194.
Fanto, M. and Mlodzik, M. (1999). Asymmetric Notch activation specifies photoreceptors R3 and R4 and planar polarity in the Drosophila eye. *Nature* **397**, 523-526.
Ferrell, J. E., Jr (2002). Self-perpetuating states in signal transduction: positive feedback, double-negative feedback and bistability. *Curr. Opin. Cell Biol.* **14**, 140-148.
Flores, G. V., Duan, H., Yan, H., Nagaraj, R., Fu, W., Zou, Y., Noll, M. and Banerjee, U. (2000). Combinatorial signaling in the specification of unique cell fates. *Cell* **103**, 75-85.
Fortini, M. E., Simon, M. A. and Rubin, G. M. (1992). Signalling by the sevenless protein tyrosine kinase is mimicked by Ras1 activation. *Nature* **355**, 559-561.
Foster, D. V., Foster, J. G., Huang, S. and Kauffman, S. A. (2009). A model of sequential branching in hierarchical cell fate determination. *J. Theor. Biol.* **260**, 589-597.
Franceschini, N., Kirschfeld, K. and Minke, B. (1981). Fluorescence of photoreceptor cells observed in vivo. *Science* **213**, 1264-1267.
Frankfort, B. J. and Mardon, G. (2004). Senseless represses nuclear transduction of Egfr pathway activation. *Development* **131**, 563-570.
Frankfort, B. J., Nolo, R., Zhang, Z., Bellen, H. and Mardon, G. (2001). senseless repression of rough is required for R8 photoreceptor differentiation in the developing Drosophila eye. *Neuron* **32**, 403-414.
Freeman, M. (1996). Reiterative use of the EGF receptor triggers differentiation of all cell types in the Drosophila eye. *Cell* **87**, 651-660.
Gabay, L., Scholz, H., Golembo, M., Klaes, A., Shilo, B. Z. and Klambt, C. (1996). EGF receptor signaling induces pointed P1 transcription and inactivates Yan protein in the Drosophila embryonic ventral ectoderm. *Development* **122**, 3355-3362.
Gardner, T. S., Cantor, C. R. and Collins, J. J. (2000). Construction of a genetic toggle switch in Escherichia coli. *Nature* **403**, 339-342.
Graf, T. and Enver, T. (2009). Forcing cells to change lineages. *Nature* **462**, 587-594.
Grimm, O., Coppey, M. and Wieschaus, E. (2010). Modelling the Bicoid gradient. *Development* **137**, 2253-2264.
Gutenkunst, R. N., Waterfall, J. J., Casey, F. P., Brown, K. S., Myers, C. R. and Sethna, J. P. (2007). Universally sloppy parameter sensitivities in systems biology models. *PLoS Comp. Biol.* **3**, 1871-1878.
Hafen, E., Basler, K., Edstroem, J. E. and Rubin, G. M. (1987). *Sevenless*, a cell-specific homeotic gene of Drosophila, encodes a putative transmembrane receptor with a tyrosine kinase domain. *Science* **236**, 55-63.
Hayashi, T., Kojima, T. and Saigo, K. (1998). Specification of primary pigment cell and outer photoreceptor fates by BarH1 homeobox gene in the developing Drosophila eye. *Dev. Biol.* **200**, 131-145.
Hayashi, T., Xu, C. and Carthew, R. W. (2008). Cell-type-specific transcription of prospero is controlled by combinatorial signaling in the Drosophila eye. *Development* **135**, 2787-2796.
Heitzler, P. and Simpson, P. (1991). The choice of cell fate in the epidermis of Drosophila. *Cell* **64**, 1083-1092.
Higashijima, S., Kojima, T., Michiue, T., Ishimaru, S., Emori, Y. and Saigo, K. (1992). Dual Bar homeo box genes of Drosophila required in two photoreceptor cells, R1 and R6, and primary pigment cells for normal eye development. *Genes Dev.* **6**, 50-60.
Hiromi, Y., Mlodzik, M., West, S. R., Rubin, G. M. and Goodman, C. S. (1993). Ectopic expression of seven-up causes cell fate changes during ommatidial assembly. *Development* **118**, 1123-1135.
Huang, S. (2009). Reprogramming cell fates: reconciling rarity with robustness. *BioEssays* **31**, 546-560.

Huang, S., Eichler, G., Bar-Yam, Y. and Ingber, D. E. (2005). Cell fates as high-dimensional attractor states of a complex gene regulatory network. *Phys. Rev. Lett.* **94**, 128701.
Huisken, J. and Stainier, D. Y. R. (2009). Selective plane illumination microscopy techniques in developmental biology. *Development* **136**, 1963-1975.
Jagla, T., Bidet, Y., Ponte, J. P. D., Dastugue, B. and Jagla, K. (2002). Cross-repressive interactions of identity genes are essential for proper specification of cardiac and muscular fates in Drosophila. *Development* **129**, 1037-1047.
Jarman, A. P., Grell, E. H., Ackerman, L., Jan, L. Y. and Jan, Y. N. (1994). Atonal is the proneural gene for Drosophila photoreceptors. *Nature* **369**, 398-400.
Jarman, A. P., Sun, Y., Jan, L. Y. and Jan, Y. N. (1995). Role of the proneural gene, atonal, in formation of Drosophila chordotonal organs and photoreceptors. *Development* **121**, 2019-2030.
Jenny, A., Darken, R. S., Wilson, P. A. and Mlodzik, M. (2003). Prickle and Strabismus form a functional complex to generate a correct axis during planar cell polarity signaling. *EMBO J.* **22**, 4409-4420.
Johnston, R. J. and Desplan, C. (2008). Stochastic neuronal cell fate choices. *Curr. Opin. Neurobiol.* **18**, 20-27.
Karim, F. D., Chang, H. C., Therrien, M., Wassarman, D. A., Laverty, T. and Rubin, G. M. (1996). A screen for genes that function downstream of Ras1 during Drosophila eye development. *Genetics* **143**, 315-329.
Kauffman, S. (1969). Homeostasis and differentiation in random genetic control networks. *Nature* **224**, 177-178.
Klein, T. J. and Mlodzik, M. (2005). Planar cell polarization: an emerging model points in the right direction. *Annu. Rev. Cell Dev. Biol.* **21**, 155-176.
Kramer, B. P. and Fussenegger, M. (2005). Hysteresis in a synthetic mammalian gene network. *Proc. Natl. Acad. Sci. USA* **102**, 9517-9522.
Kuhlman, T., Zhang, Z., Saier, M. H. and Hwa, T. (2007). Combinatorial transcriptional control of the lactose operon of Escherichia coli. *Proc. Natl. Acad. Sci. USA* **104**, 6043-6048.
Lai, Z. C. and Rubin, G. M. (1992). Negative control of photoreceptor development in Drosophila by the product of the *yan* gene, an ETS domain protein. *Cell* **70**, 609-620.
Laslo, P., Spooner, C., Warmflash, A., Lancki, D., Lee, H., Sciammas, R., Gantner, B., Dinner, A. R. and Singh, H. (2006). Multilineage transcriptional priming and determination of alternate hematopoietic cell fates. *Cell* **126**, 755-766.
Laslo, P., Pongubala, J. M. R., Lancki, D. W. and Singh, H. (2008). Gene regulatory networks directing myeloid and lymphoid cell fates within the immune system. *Semin. Immunol.* **20**, 228-235.
Lawrence, P. A., Struhl, G. and Casal, J. (2007). Planar cell polarity: one or two pathways? *Nat. Rev. Genet.* **8**, 555-563.
Lawrence, P. A., Struhl, G. and Casal, J. (2008). Planar cell polarity: a bridge too far? *Curr. Biol.* **18**, 959-961.
Le Garrec, J.-F. and Kerszberg, M. (2008). Modeling polarity buildup and cell fate decision in the fly eye: insight into the connection between the PCP and Notch pathways. *Dev. Genes Evol.* **218**, 413-426.
Le Garrec, J.-F., Lopez, P. and Kerszberg, M. (2006). Establishment and maintenance of planar epithelial cell polarity by asymmetric cadherin bridges: a computer model. *Dev. Dyn.* **235**, 235-246.
Li, S., Li, Y., Carthew, R. W. and Lai, Z. C. (1997). Photoreceptor cell differentiation requires regulated proteolysis of the transcriptional repressor Tramtrack. *Cell* **90**, 469-478.
Li, X. and Carthew, R. W. (2005). A microRNA mediates EGF receptor signaling and promotes photoreceptor differentiation in the Drosophila eye. *Cell* **123**, 1267-1277.
Li, X., Cassidy, J. J., Reinke, C. A., Fischboeck, S. and Carthew, R. W. (2009). A microRNA imparts robustness against environmental fluctuation during development. *Cell* **137**, 273-282.
Lohmueller, J., Neretti, N., Hickey, B., Kaka, A., Gao, A., Lemon, J., Lattanzi, V., Goldstein, P., Tam, L. K., Schmidt, M. et al. (2007). Progress toward construction and modelling of a tri-stable toggle switch in E. coli. *Synth. Biol.* **1**, 25-28.
Lopes, F. J., Vieira, F. M., Holloway, D. M., Bisch, P. M. and Spirov, A. V. (2008). Spatial bistability generates hunchback expression sharpness in the Drosophila embryo. *PLoS Comput. Biol.* **4**, e1000184.
Lucchetta, E. M., Lee, J. H., Fu, L. A., Patel, N. H. and Ismagilov, R. F. (2005). Dynamics of Drosophila embryonic patterning network perturbed in space and time using microfluidics. *Nature* **434**, 1134-1138.
Lucchetta, E. M., Carthew, R. W. and Ismagilov, R. F. (2009). The endo-siRNA pathway is essential for robust development of the Drosophila embryo. *PLoS ONE* **4**, e7576.
Meinhardt, H. (2008). Models of biological pattern formation: from elementary steps to the organization of embryonic axes. *Curr. Top. Dev. Biol.* **81**, 1-63.
Meissner, A., Mikkelsen, T. S., Gu, H., Wernig, M., Hanna, J., Sivachenko, A., Zhang, X., Bernstein, B. E., Nusbaum, C., Jaffe, D. B. et al. (2008). Genome-scale DNA methylation maps of pluripotent and differentiated cells. *Nature* **454**, 766-770.
Mikeladze-Dvali, T., Wernet, M. F., Pistillo, D., Mazzoni, E. O., Teleman, A. A., Chen, Y.-W., Cohen, S. and Desplan, C. (2005). The growth regulators warts/lats and melted interact in a bistable loop to specify opposite fates in Drosophila R8 photoreceptors. *Cell* **122**, 775-787.
Mikkelsen, T. S., Ku, M., Jaffe, D. B., Issac, B., Lieberman, E., Giannoukos, G., Alvarez, P., Brockman, W., Kim, T. K., Koche, R. P. et al. (2007). Genome-wide maps of chromatin state in pluripotent and lineage-committed cells. *Nature* **448**, 553-560.
Miller, A. C., Seymour, H., King, C. and Herman, T. G. (2008). Loss of seven-up from Drosophila R1/R6 photoreceptors reveals a stochastic fate choice that is normally biased by Notch. *Development* **135**, 707-715.
Mlodzik, M., Hiromi, Y., Weber, U., Goodman, C. S. and Rubin, G. M. (1990). The Drosophila *seven-up* gene, a member of the steroid receptor gene superfamily, controls photoreceptor cell fates. *Cell* **60**, 211-224.
Monod, J. and Jacob, F. (1961). General conclusions: teleonomic mechanisms in cellular metabolism, growth, and differentiation. *Cold Spring Harbor Symp. Quant. Biol.* **26**, 389-401.
Montell, D. J. (2008). Morphogenetic cell movements: diversity from modular mechanical properties. *Science* **322**, 1502-1505.
Morante, J., Desplan, C. and Celik, A. (2007). Generating patterned arrays of photoreceptors. *Curr. Opin. Genet. Dev.* **17**, 314-319.
Moses, K. (2002). *Drosophila Eye Development: Results and Problems in Cell Differentiation.* Heidelberg: Springer.
Novick, A. and Weiner, M. (1957). Enzyme induction as an all-or-none phenomenon. *Proc. Natl. Acad. Sci. USA* **43**, 553-566.
Oates, A. C., Gorfinkiel, N., González-Gaitán, M. and Heisenberg, C.-P. (2009). Quantitative approaches in developmental biology. *Nat. Rev. Genet.* **10**, 517-530.
O'Neill, E. M., Rebay, I., Tjian, R. and Rubin, G. M. (1994). The activities of two Ets-related transcription factors required for Drosophila eye development are modulated by the Ras/MAPK pathway. *Cell* **78**, 137-147.
Pennington, M. W. and Lubensky, D. K. (2010). Switch and template pattern formation in a discrete reaction diffusion system inspired by the Drosophila eye. *Quant. Biol.* (in press).
Pepple, K. L., Atkins, M., Venken, K., Wellnitz, K., Harding, M., Frankfort, B. and Mardon, G. (2008). Two-step selection of a single R8 photoreceptor: a bistable loop between senseless and rough locks in R8 fate. *Development* **135**, 4071-4079.
Pickup, A. T., Ming, L. and Lipshitz, H. D. (2009). Hindsight modulates Delta expression during Drosophila cone cell induction. *Development* **136**, 975-982.
Ptashne, M. (2004). *A Genetic Switch: Phage Lambda Revisited.* Cold Spring Harbor, NY: Cold Spring Harbor Laboratory Press.
Qiao, F., Song, H., Kim, C. A., Sawaya, M. R., Hunter, J. B., Gingery, M., Courey, A. J., Rebay, I. and Bowie, J. U. (2004). Derepression by depolymerization: structural insights into the regulation of Yan by Mae. *Cell* **118**, 163-173.
Ready, D. F., Hanson, T. E. and Benzer, S. (1976). Development of the Drosophila retina, a neurocrystalline lattice. *Dev. Biol.* **53**, 217-240.
Rebay, I. and Rubin, G. M. (1995). Yan functions as a general inhibitor of differentiation and is negatively regulated by activation of the Ras1/MAPK pathway. *Cell* **81**, 857-866.
Reinitz, J. and Vaisnys, J. R. (1990). Theoretical and experimental analysis of the phage lambda genetic switch implies missing levels of co-operativity. *J. Theor. Biol.* **145**, 295-318.
Rohrbaugh, M., Ramos, E., Nguyen, D., Price, M., Wen, Y. and Lai, Z. C. (2002). Notch activation of yan expression is antagonized by RTK/Pointed signaling in the Drosophila eye. *Curr. Biol.* **12**, 576-581.
Roignant, J.-Y. and Treisman, J. E. (2009). Pattern formation in the Drosophila eye disc. *Int. J. Dev. Biol.* **53**, 795-804.
Rosenfeld, N., Young, J. W., Alon, U., Swain, P. S. and Elowitz, M. B. (2005). Gene regulation at the single-cell level. *Science* **307**, 1962-1965.
Saiz, L., Rubi, J. M. and Vilar, J. M. G. (2005). Inferring the in vivo looping properties of DNA. *Proc. Natl. Acad. Sci. USA* **102**, 17642-17645.
Santillán, M. and Mackey, M. C. (2004). Why the lysogenic state of phage lambda is so stable: a mathematical modeling approach. *Biophys. J.* **86**, 75-84.
Setty, Y., Mayo, A. E., Surette, M. G. and Alon, U. (2003). Detailed map of a cis-regulatory input function. *Proc. Natl. Acad. Sci. USA* **100**, 7702-7707.
Shi, Y. and Noll, M. (2009). Determination of cell fates in the R7 equivalence group of the Drosophila eye by the concerted regulation of D-Pax2 and TTK88. *Dev. Biol.* **331**, 68-77.
Sick, S., Reinker, S., Timmer, J. and Schlake, T. (2006). WNT and DKK determine hair follicle spacing through a reaction-diffusion mechanism. *Science* **314**, 1447-1450.
Siegal-Gaskins, D., Grotewold, E. and Smith, G. D. (2009). The capacity for multistability in small gene regulatory networks. *BMC Syst. Biol.* **3**, 96.
Sprinzak, D., Lakhanpal, A., Lebon, L., Santat, L. A., Fontes, M. E., Anderson, G. A., Garcia-Ojalvo, J. and Elowitz, M. B. (2010). Cis-interactions between Notch and Delta generate mutually exclusive signalling states. *Nature* **465**, 86-90.
Strutt, D., Johnson, R., Cooper, K. and Bray, S. (2002). Asymmetric localization of frizzled and the determination of notch-dependent cell fate in the Drosophila eye. *Curr. Biol.* **12**, 813-824.

Strutt, H. and Strutt, D. (2008). Differential stability of flamingo protein complexes underlies the establishment of planar polarity. *Curr. Biol.* **18**, 1555-1564.
Strutt, H. and Strutt, D. (2009). Asymmetric localisation of planar polarity proteins: mechanisms and consequences. *Semin. Cell Dev. Biol.* **20**, 957-963.
Swanson, C. I., Evans, N. C. and Barolo, S. (2010). Structural rules and complex regulatory circuitry constrain expression of a Notch- and EGFR-regulated eye enhancer. *Dev. Cell* **18**, 359-370.
Teleman, A. A., Chen, Y.-W. and Cohen, S. M. (2005). Drosophila Melted modulates FOXO and TOR activity. *Dev. Cell* **9**, 271-281.
Tomlinson, A. and Ready, D. F. (1987). Cell fate in the drosophila ommatidium. *Dev. Biol.* **123**, 264-275.
Tomlinson, A. and Struhl, G. (2001). Delta/Notch and Boss/Sevenless signals act combinatorially to specify the Drosophila R7 photoreceptor. *Mol. Cell* **7**, 487-495.
Tootle, T. L., Lee, P. S. and Rebay, I. (2003). CRM1-mediated nuclear export and regulated activity of the receptor tyrosine kinase antagonist YAN require specific interactions with MAE. *Development* **130**, 845-857.
Turing, A. M. (1952). The chemical basis of morphogenesis. *Philos. Trans. R. Soc. Lond. B Biol. Sci.* **237**, 37-72.
Umulis, D. M., Serpe, M., O'Connor, M. B. and Othmer, H. G. (2006). Robust, bistable patterning of the dorsal surface of the Drosophila embryo. *Proc. Natl. Acad. Sci. USA* **103**, 11613-11618.
Venken, K. J. T., He, Y., Hoskins, R. A. and Bellen, H. J. (2006). P[acman]: a BAC transgenic platform for targeted insertion of large DNA fragments in D. melanogaster. *Science* **314**, 1747-1751.
Vinegoni, C., Razansky, D., Pitsouli, C., Perrimon, N., Ntziachristos, V. and Weissleder, R. (2009). Mesoscopic fluorescence tomography for in-vivo imaging of developing Drosophila. *J. Vis. Exp.* **30**, 1510.
Vivekanand, P., Tootle, T. L. and Rebay, I. (2004). MAE, a dual regulator of the EGFR signaling pathway, is a target of the Ets transcription factors PNT and YAN. *Mech. Dev.* **121**, 1469-1479.
Voas, M. G. and Rebay, I. (2004). Signal integration during development: insights from the Drosophila eye. *Dev. Dyn.* **229**, 162-175.
Waddington, C. H. (1957). *The Strategy of The Genes: A Discussion of Some Aspects of Theoretical Biology.* London: Allen and Unwin.
Wang, L., Walker, B. L., Iannaccone, S., Bhatt, D., Kennedy, P. J. and Tse, W. T. (2009). Bistable switches control memory and plasticity in cellular differentiation. *Proc. Natl. Acad. Sci. USA* **106**, 6638-6643.
Wang, Y.-C. and Ferguson, E. L. (2005). Spatial bistability of Dpp-receptor interactions during Drosophila dorsal-ventral patterning. *Nature* **434**, 229-234.
Warmflash, A. and Dinner, A. R. (2009). Modeling gene regulatory networks for cell fate specification. In *Statistical Mechanics of Cellular Systems and Processes* (ed. M. H. Zaman), pp. 121-154. Cambridge: Cambridge University Press.
Wernet, M. F., Mazzoni, E. O., Celik, A., Duncan, D. M., Duncan, I. and Desplan, C. (2006). Stochastic spineless expression creates the retinal mosaic for colour vision. *Nature* **440**, 174-180.
Wong, P., Gladney, S. and Keasling, J. D. (1997). Mathematical model of the greater operon: inducer exclusion, catabolite repression, and diauxic growth on glucose and lactose. *Biotech. Progress* **13**, 132-143.
Xu, C., Kauffmann, R. C., Zhang, J., Kladny, S. and Carthew, R. W. (2000). Overlapping activators and repressors delimit transcriptional response to receptor tyrosine kinase signals in the Drosophila eye. *Cell* **103**, 87-97.
Yan, S.-J., Zartman, J. J., Zhang, M., Scott, A., Shvartsman, S. Y. and Li, W. X. (2009). Bistability coordinates activation of the EGFR and DPP pathways in Drosophila vein differentiation. *Mol. Syst. Biol.* **5**, 278.
Yang, C.-h., Axelrod, J. D. and Simon, M. A. (2002). Regulation of Frizzled by fat-like cadherins during planar polarity signaling in the Drosophila compound eye. *Cell* **108**, 675-688.
Yao, G., Lee, T. J., Mori, S., Nevins, J. R. and You, L. (2008). A bistable Rb-E2F switch underlies the restriction point. *Nat. Cell Biol.* **10**, 476-482.
Zhang, J., Graham, T. G. W., Vivekanand, P., Cote, L., Cetera, M. and Rebay, I. (2010). Sterile alpha motif domain-mediated self-association plays an essential role in modulating the activity of the Drosophila ETS family transcriptional repressor Yan. *Mol. Cell. Biol.* **30**, 1158-1170.
Zheng, L., Zhang, J. and Carthew, R. W. (1995). frizzled regulates mirror-symmetric pattern formation in the Drosophila eye. *Development* **121**, 3045-3055.

Table S1. Gene regulation parameters giving bistable behavior of the Yan network model

Yan expression	p_{1mY}	0.4
	p_{2mY}	0.4
	p_{3mY}	0.2
	k_{mY}	0.1
	e_{mY}	0.2
	α_{mY}	–0.2
	n_{mY}	2
PntP1 expression	p_{1P_1}	0.5
	p_{2P_1}	0.5
	k_{P_1}	0.1
	e_{P_1}	0.01
	α_{P_1}	0.19
	n_{P_1}	2
	k'_{P_1}	0.1
	n'_{P_1}	2
PntP2 expression	e_{P_2}	0.1
Mae expression	p_{1M}	0.5
	p_{2M}	0.5
	k_M	0.1
	e_M	0.01
	α_M	0.19
	n_M	2
	k'_M	0.1
	n'_M	2
miR-7 expression	p_{1mR7}	0.5
	p_{2mR7}	0.5
	k_{mR7}	0.1
	e_{mR7}	0.01
	α_{mR7}	0.19
	n_{mR7}	2
	k'_{mR7}	0.1
	n'_{mR7}	2

yan mRNA was translated at rate k^t_Y=0.1.

Table S2. Degradation rates giving bistable behavior of the Yan network model

yan mRNA	d_{mY}	0.1
Yan protein	d_Y	0.1
phospho-Yan	d_{Y^*}	10
PntP1	d_{P_1}	0.1
PntP2	d_{P_2}	0.1
phospho-PntP2	$d_{P_2^*}$	0.1
Mae	d_M	0.1
Mae-Yan complex	$d_{M:Y}$	0.1
Mae–phospho-Yan complex	$d_{M:Y^*}$	0.1
Mae-PntP2	$d_{M:P_2}$	0.1
miR-7	d_{mR7}	0.1
yan mRNA-miR-7 complex	$d_{mY:mR7}$	0.1

Table S3. Binding and unbinding rates giving bistable behavior of the Yan network model

Mae-Yan association	$\vec{k}_{M:Y}$	0.1
Mae-Yan dissociation	$\overleftarrow{k}_{M:Y}$	0.01
Mae–phospho-Yan association	$\vec{k}_{M:Y*}$	0.1
Mae–phospho-Yan dissociation	$\overleftarrow{k}_{M:Y*}$	10
Mae-PntP2 association	$\vec{k}_{M:P_2}$	0.1
Mae-PntP2 dissociation	$\overleftarrow{k}_{M:P_2}$	0.01
yan mRNA-miR-7 association	$\vec{k}_{m_{R7}}$	0.1
yan mRNA-miR-7 dissociation	$\overleftarrow{k}_{m_{R7}}$	0.01

Table S4. Kinase Michaelis-Menten parameters giving bistable behavior of the Yan network model

k_{cat} for Yan phosphorylation	α_{Y^*}	0.1
K_m for Yan phosphorylation	K_{Y^*}	0.1
k_{cat} for PntP2 phosphorylation	$\alpha_{P_2^*}$	0.1
K_m for PntP2 phosphorylation	$K_{P_2^*}$	0.1